

MIGMA IV HIGH ENERGY FUSION APPARATUS

J. Ferrer, R. Ho, M. Mazarakis, S. Mensian,
J. Nering, C. Powell, J. Sandberg, J. Treglio, B. Maglich

Fusion Energy Corporation
Princeton, New Jersey 08540

In order to study the scattering-dominated regime in a migma high energy fusion device, several improvements have been made to the experimental apparatus. The injected beam current has been increased; protective systems and cooled beam stops have been installed to handle the beam power. The migma diagnostics include rf pickup electrodes for continuous monitoring of orbit distributions, silicon surface barrier detectors for observation of fusion products in coincidence and a charge-exchange neutral particle detector. The apparatus is shown in Figures 1 and 2.

Earlier experiments with Migma III achieved a stored ion number of 2×10^9 ; ion lifetimes of 2 sec were observed with background gas pressures of 10^{-7} torr. The recent modifications have resulted in a five-fold increase in injected beam current and a simultaneous improvement of two orders of magnitude in vacuum conditions. A cooled copper beamstop makes possible the disposal of the untrapped beam. Steady state background gas pressures of 10^{-9} torr are observed during injection of a 740 watt D_2^+ beam.

In the case of Migma III, the primary trapping mechanism was Lorentz dissociation of the injected D_2^+ ions. In Migma IV, however, collisional dissociation of the injected beam on the already trapped ions will become the dominant source of migma ions. The collisional dissociation process will tend to produce an initial migma ion distribution strongly peaked at small impact parameters and at the midplane of the chamber. At the resultant densities, scattering will become an important process; the distribution will tend to spread, particularly in the axial direction.

Preliminary experiments with the Migma IV chamber have yielded enough information to make the calculation of steady-state parameters possible. A D_2^+ current in excess of 500 μA can be routinely injected into the chamber. After a brief period of outgassing, the pressure falls into the 10^{-9} torr range (titanium sublimators in operation and LN_2 torus filled). During a typical test, the pressure fell to 10^{-9} torr after about one hour of dc beam injection; the vacuum was still improving when the test was terminated. The beam diameter was less than 3/16" (the size of the tungsten axial probe). The background gas consisted of H_2 and D_2 in approximately equal amounts with a small (5%) amount of HD. No other peaks were observed on the residual gas analyzer. The vacuum measuring setup was essentially the same as was used with Migma III with the exception that a residual gas analyzer has been added to the system.

For the purposes of simulation, the following conservative parameters are taken:

Injected beam — 300 μA D_2^+ @ 1.35 MeV
Beam diameter — 0.5 cm
Background gas — 10^{-9} torr Hydrogen

These parameters and those describing the Migma IV chamber and magnetic field were used with the FEC self-consistent three dimensional Monte-Carlo simulation program to determine the anticipated operating regime for Migma IV. The computer program accounts for all relevant classical ion-ion and ion-electron processes as well as charge exchange with the background gas. The program has no ability to predict stability properties of the stored ions.

Table 1 gives the most significant Migma IV parameters resulting from the simulation. Two dimensional distributions of density and fusing ions are shown in Figure 3.

The wall-imposed mirror ratio (1.02) accounts for the high ratio of scattering to fusion. However, even in Migma IV the fusion rate from migma-migma collisions ($1.8 \times 10^9 \text{ sec}^{-1}$) will be sufficient to produce optimum count rates in the silicon surface barrier detectors used to analyze fusion events.

From the computer generated parameters, it may be easily verified that the conditions for exponentiation to the scattering dominated regime exist in Migma IV. The collisional dissociation rate per trapped ion is approximately 3.5 times the charge transfer rate per trapped ion. Increasing the beam current to 500 μA (at which the assumed vacuum conditions have been demonstrated) will further improve this parameter.

TABLE 1

Beam	300 μA , 1.35 MeV D_2^+
Beam Diameter	.5 cm
Background gas	10^{-9} torr Hydrogen
Central field	3.4 T
Effective Mirror ratio	1.02 (wall-imposed)
Chamber height	8 cm
Total Number of Stored Particles	10^{14}
Density of Stored Particles	$5 \times 10^{10} \text{ cm}^{-3}$
Charge Transfer time	140 sec.
Scattering time	57 sec.
Fusion time	$5.5 \times 10^4 \text{ sec.}$
Average ion lifetime	40 sec.
Collisionally trapped beam fraction	.14%

- 1 Analyzing Magnet
- 2 (A/B) Gas Valve
- 3 H₂ Silt Aperture
- 4 Silt Assembly
- 5 Beam Switcher
- 6 H₂O Coated Protective Aperture 25°
- 7 Ceramic Vacuum Breaks
- 8 Gas Valve L1
- 9 Front Coated Insulated Aperture 1°
- 10 Faraday Cup F1
- 11 Trigger Group
- 12 H₂O Coated Protective Aperture 10°
- 13 Elec. Quadrupole Triple Lens Q₃
- 14 Electronic Beam Steerer
- 15 Chamber Gas Valve
- 16 Front Coated Aperture 200°
- 17 Faraday Cup 200°
- 18 Residual Gas Analyzer
- 19 Vacuum-Jacked Pumping Manifold
- 20 L₁ Chamber Reservoir
- 21 Subconducting Mag. Power Transformer
- 22 Crystal Pressure Gauge
- 23 L₁ Shield Pin
- 24 Copper FN Tube
- 25 Crystal Safety Blow Off
- 26 Supracon. Mag. Conductor Lens
- 27 L₁ Shield Vent
- 28 Support Pin Structure
- 29 Neutral Particle Detector
- 30 Vent and Roughing Valve
- 31 Viewing Port
- 32 Front Coated Aperture 0°
- 33 Faraday Cup 0°
- 34 Vacuum Subdivisor
- 35 Radial Scraper
- 36 Supracon. Mag. Chamber Support
- 37 Thermal Mechanical Lock
- 38 Helium Chamber
- 39 Central Lens Gas Barbs
- 40 Superconducting Magnet
- 41 Acid Probe
- 42 L₁2 Tracer Tube Vent
- 43 Detector Amplifiers
- 44 Dimensional Diff Pump
- 45 L₁2 Trap
- 46 H₂ Pump
- 47 Ferrous Thermocouple Gauge
- 48 Fore Pump
- 49 Upstream Diff Pump
- 50 Roughing Valve
- 51 Pneumatic Valve
- 52 O Ring Heater
- 53 Hot Off Flow Gauge
- 54 Expansion Jeld Cryo-Tone
- 55 Vacuum-Jacked Thermocouple Gauge

(see details for 3,4,5,6,10,13,14)

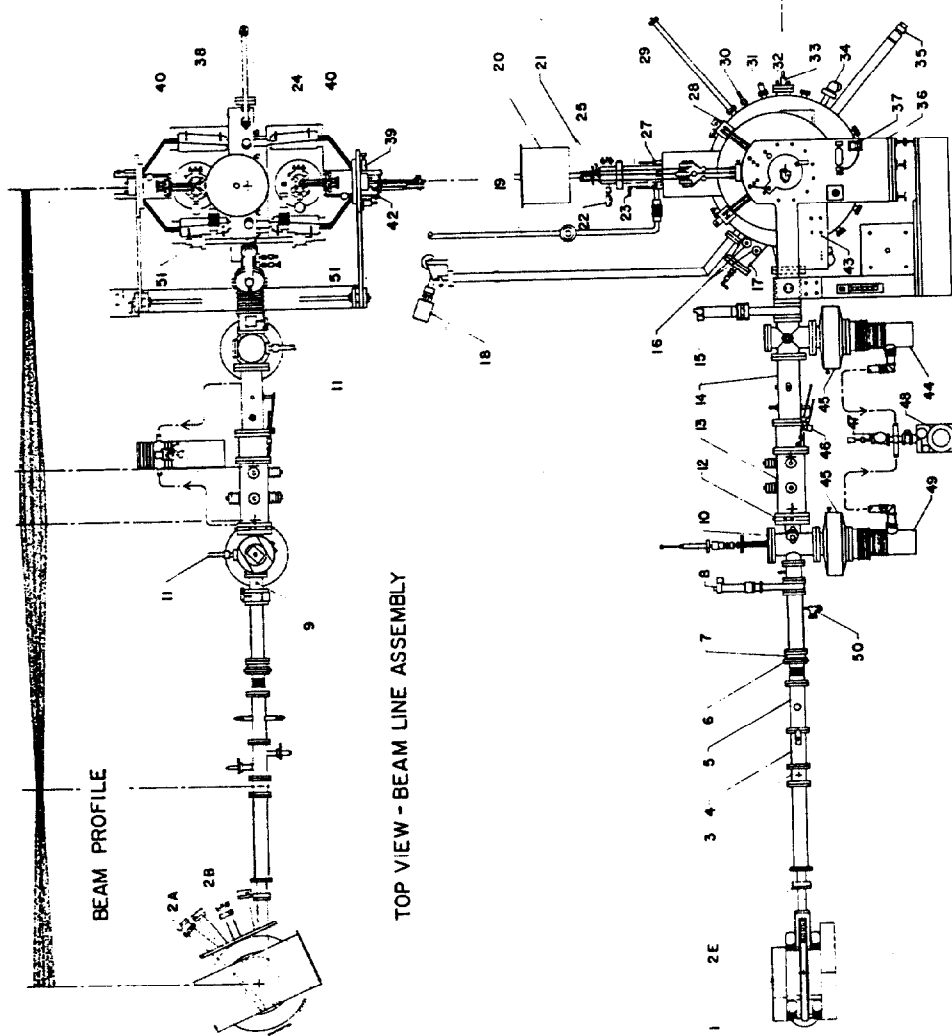


FIGURE 1. BEAMLINE AND MIGMA IV CHAMBER

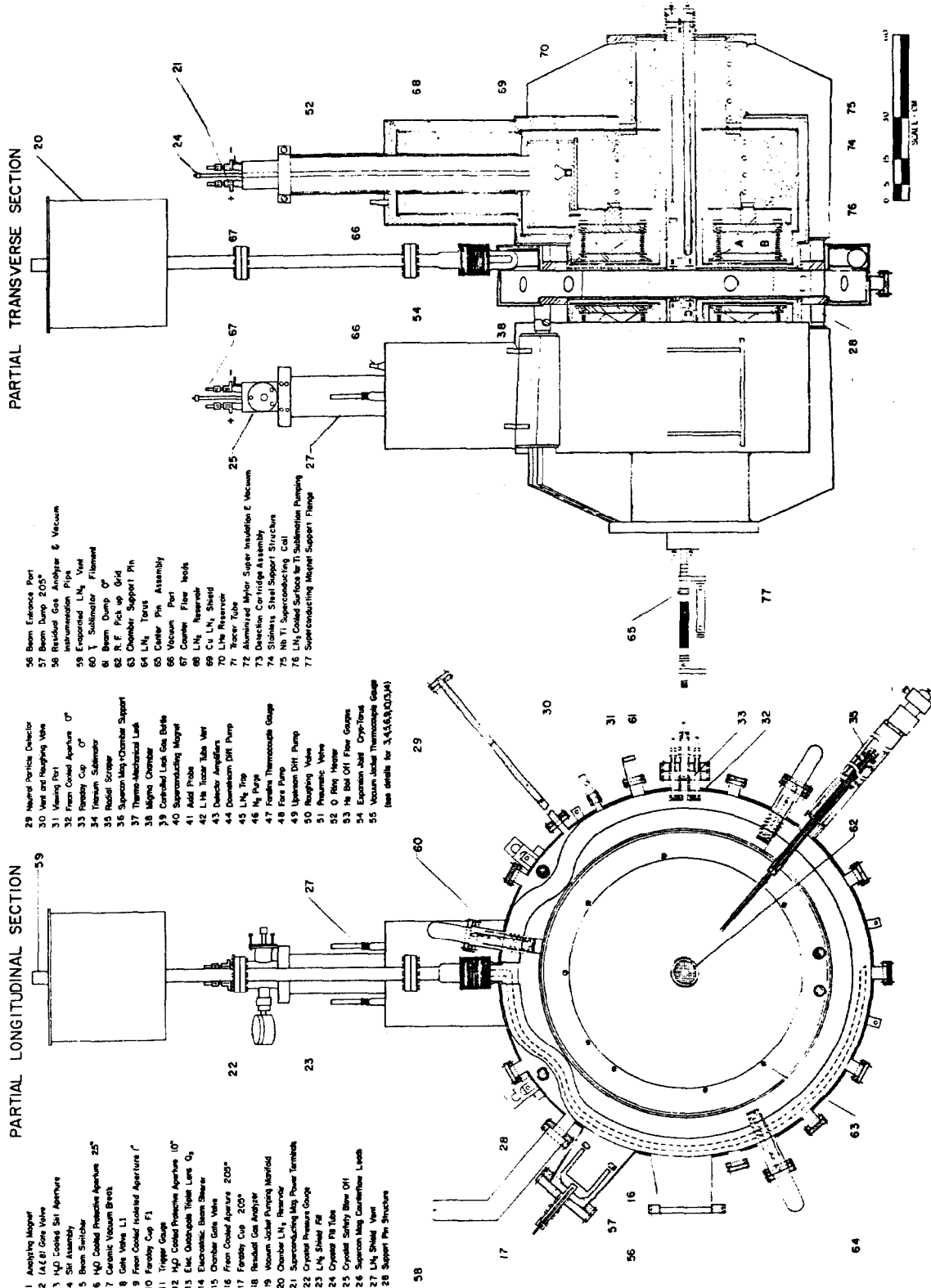


FIGURE 2. MAGMA IV CHAMBER AND SUPERCONDUCTING MAGNET

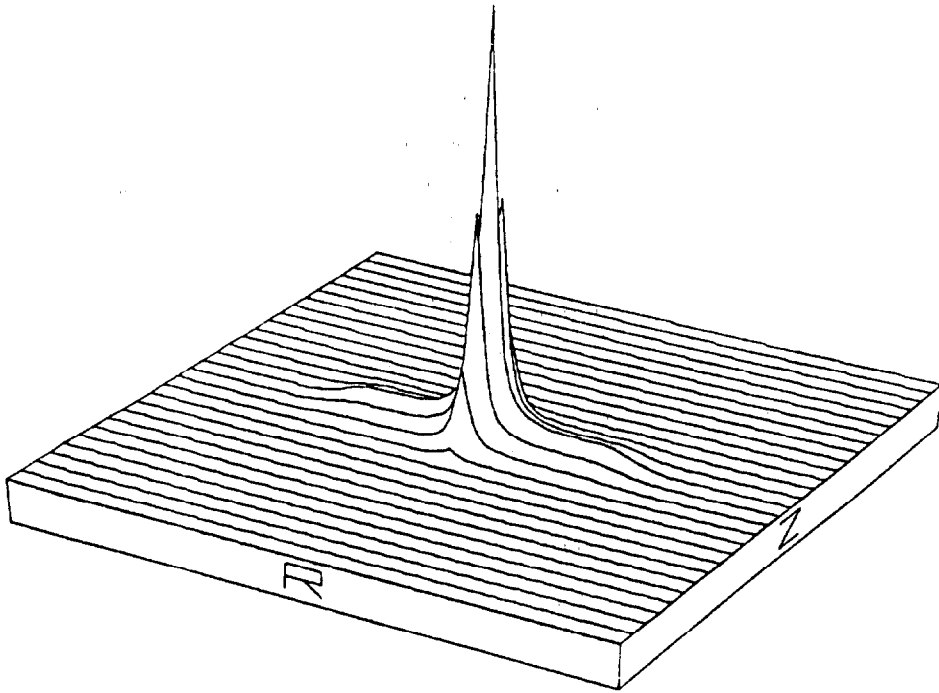


FIGURE 3a. DENSITY AS A FUNCTION OF POSITION (R, Z)

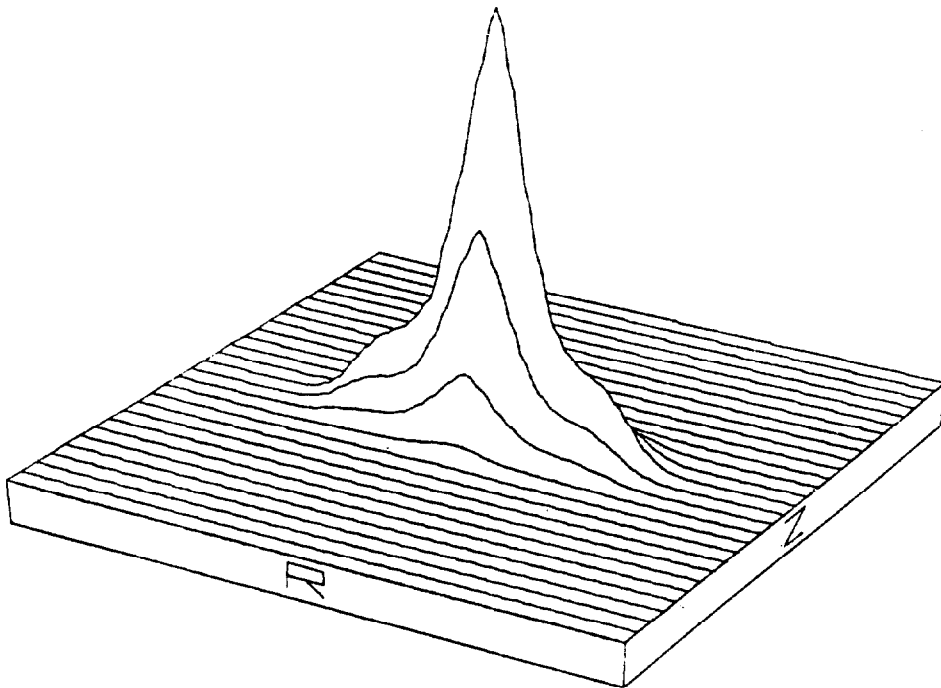


FIGURE 3b. NUMBER OF FUSIONS AS A FUNCTION OF POSITION $(R, Z,)$